Conformational Change of Phenyl Ring Side Group during Stress Relaxation in Glassy Poly(styrene-*co*-acrylonitrile)

Shinya Takahashi and Hiromu Saito*

Department of Organic and Polymer Materials Chemistry, Tokyo University of Agriculture and Technology, Koganei-shi, Tokyo 184-8588, Japan

Received September 28, 2003; Revised Manuscript Received November 22, 2003

ABSTRACT: We investigated the stress and birefringence Δn during stress relaxation in poly(styrene-*co*-acrylonitrile). The Δn changed its sign from positive to negative during the stress relaxation with increasing relaxation time and temperature in the glassy region. The negative Δn was found to increase when the stress was released and the specimen was cooled to room temperature. Such characteristic Δn behavior is ascribed to three relaxation mechanisms consisting of distortion, orientation, and conformational change of the phenyl ring side group. The master curve of the Δn was nicely explained by assuming that the distortion relaxation is expressed by Kohlrausch−Williams−Watts equation, the orientation relaxation by modified Rouse equation, and the conformational change by a stretched exponential relaxation function. The curve fitting procedures of the master curves revealed that the conformational change of the side group is much slower than the phenyl ring vibration (β relaxation); i.e., the rotational angle of the side group changes from 28° to 48° with a relaxation time of 0.15 s (at 105 °C) during the stress relaxation.

Introduction

Stress and birefringence are induced when glassy amorphous polymers are deformed. Both stress and birefringence originated from two contributions: distortion and orientation.[1−4] The distortion is local change of the intersegment distance by torsion around the main-chain bonds or local displacement of the interchain spacing. On the other hand, the orientation is relatively long-range conformational rearrangements by molecular orientation of the main-chain segments. The distortion and orientation are relaxed during the stress relaxation. The photoelastic law suggests that the birefringence is proportional to the stress.[5] Hence, the stress−optical coefficient, which is obtained by the ratio of birefringence to stress, is constant with time and/or temperature during the stress relaxation in glassy noncrystalline polymers such as polycarbonate.

The stress−optical coefficient changes its sign from positive to negative with increasing relaxation time and/or temperature in glassy styrenic polymers during the stress relaxation.[6,7] Such characteristic relaxation behavior is explained by taking into account the conformational change of the phenyl ring side group.[8,9] On the other hand, two relaxation modes for the phenyl ring side group are suggested by a series of the relaxation studies such as mechanical relaxation,[10−12] dielectric relaxation,[12,13] nuclear magnetic resonance,[14−18] and neutron scattering.[19,20] One of the relaxation modes is γ-relaxation observed at around −100 °C.[12,13,19,20] The γ-relaxation is assigned to the phenyl ring π (180°) flip motion having the relaxation time of 10^{-7}−10^{-8} s.[15−18] The other is β-relaxation observed at around 50 °C, and the relaxation time is 10^{-4} s.[11−15] The β-relaxation is assigned to the phenyl ring vibration which is cooperative with the main-chain vibration. The observed temperature for the β-relaxation is close to the temperature in which the stress−optical coefficient changes its sign. However, the conformational change and the relation to the β-relaxation have not been clarified.

In this paper, to understand the conformational change, we carry out the simultaneous measurement of stress and birefringence as a function of relaxation time after uniaxial stretching of poly(styrene-*co*-acrylonitrile) (SAN) film over a wide temperature region. The results of the relaxation behavior are quantitatively discussed in terms of the Kohlrausch−Williams−Watts equation for the distortion relaxation, the modified Rouse equation for the orientation relaxation, and a stretched exponential function for the conformational change.

Experimental Section

Poly(styrene-*co*-acrylonitrile) (SAN) pellet was supplied by Tosoh Co., Ltd. The weight-average molecular weight was 10.0 × 10^4, and the acrylonitrile content was 30 wt %. The pellet was compression molded at 200 °C into a film about 0.2 mm thick. The film was then cut into a rectangule of length 50 mm and width 5 mm.

Figure 1 shows an apparatus for the simultaneous measurement of stress σ and birefringence Δn. In the tensile testing system (Far-East Manufacturing Inc.), two cross heads traveled up and down at the same speed so that the light beam for Δn measurement irradiated the midpoint of the specimen throughout the stretching and relaxation processes. The specimen was quickly stretched (90 mm/s) up to a draw ratio ϵ of 1.005 below the glass transition temperature T_g and ϵ of 1.01 above the T_g. The measurement was carried out at various temperatures in the range from 30 to 125 °C. The data of stress were processed by a personal computer through an A/D converter. The modulus E was obtained by $E = \sigma/\epsilon$.

Precise measurement of the birefringence was carried out using a photoelastic modulator (PEM).[21−23] A 632.8 nm He−Ne laser beam was passed through a Gran-Thomson polarizer and PEM (ADR-200, ORC Manufacturing Co., Ltd.). The PEM produced a sinusoidal retardation $\delta_0 = A \sin(\omega t)$ with high frequency (ω = 50 kHz) and adjustable amplitude A, and then the modulated light was applied to the specimen. After passing through a Gran-Thomson analyzer, the light was detected by a photodiode. The retardation R by the specimen is given by

* Corresponding author: e-mail hsaitou@cc.tuat.ac.jp.

10.1021/ma035458a CCC: $27.50
Published on Web 01/08/2004

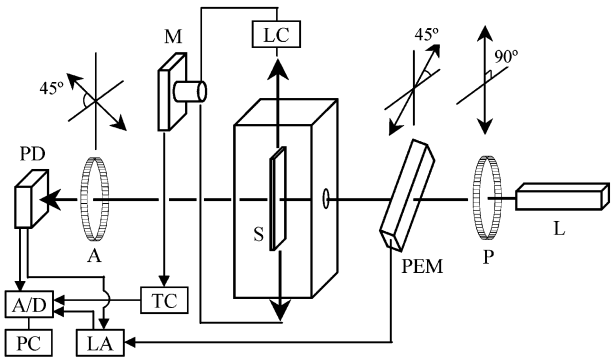

Figure 1. Apparatus for simultaneous measurements of stress and birefringence: L, laser; P, polarizer; PEM, photoelastic modulator; S, specimen; LC, load cell; M, motor; A, analyzer; PD, photodiode; TC, tensile controller; LA, lock-in amplifier; A/D, A/D converter; PC, personal computer.

$$R = \sin^{-1}[E_{AC}/\{2J_1(\delta_0)E_{DC}\}] \quad (1)$$

where E_{AC} and E_{DC} are AC and DC amplitudes of detected light, respectively, and $J_1(\delta_0)$ is the first Bessel function which is experimentally determined as a calibration constant. Then the birefringence Δn is given by

$$\Delta n = (R\lambda d)/2\pi \quad (2)$$

where λ is the wavelength of light and d is the thickness of the specimen.

Results and Discussion

Figure 2 shows the time dependence of the relaxation modulus $E(t)$ and relaxation birefringence $\Delta n(t)/\epsilon$ of SAN at various temperatures. The $E(t)$ is almost constant with time t in the glassy region (below 50 °C), and it decreases steeply in the glass transition region (80−100 °C). This is typical for the modulus relaxation behavior of noncrystalline polymers. On the other hand, the $\Delta n(t)/\epsilon$ shows a characteristic relaxation behavior. The $\Delta n(t)/\epsilon$ is initially positive, decreases to attain zero, changes its sign from positive to negative, and then decreases with time at temperature between 50 and 90 °C. The onset time for the change of the sign becomes shorter with increasing temperature. At high temperature above 100 °C, the $\Delta n(t)/\epsilon$ is negative throughout the relaxation time.

The $E(t)$ curves obtained at various temperatures could be superimposed to a master curve by a horizontal shift. The master curve $E(t/a_T)$ reduced at a reference temperature, where a_T is the shift factor, is shown in Figure 3a. Here, the reference temperature is the glass transition temperature T_g of SAN: 105 °C. The temperature dependence of the shift factor $a_T(T)$ is shown in the inset of Figure 3a. The $a_T(T)$ followed the Vogel−Fulcher equation[24] above the T_g, as shown by a solid line in the inset of Figure 3a. The observed $a_T(T)$ is deviated from the calculated curve by the Vogel−Fulcher equation at the temperature below the T_g. The deviation may be explained by the change of relaxation modes from the collective molecular motion above the T_g to the local segmental motion below the T_g.[25,26]

The $\Delta n(t)/\epsilon$ curves obtained at various temperatures could be also superimposed to a master curve by using the $a_T(T)$ for the $E(t/a_T)$ demonstrated in the inset of Figure 3a. The master curve $\Delta n(t/a_T)/\epsilon$ thus obtained is shown in Figure 3b. The interesting result in Figure 3 is that the $\Delta n(t/a_T)/\epsilon$ changes its sign from positive to negative in the glassy region in which the $E(t/a_T)$ is almost constant with relaxation time and/or temperature. The $E(t/a_T)$ shows a clear inflection at the onset t/a_T of the rubbery plateau region. On the other hand, the inflection is not clear in the $\Delta n(t/a_T)/\epsilon$. The difference may be ascribed to the two molecular mechanisms for the relaxation and the different contributions to the $E(t/a_T)$ and $\Delta n(t/a_T)/\epsilon$, as discussed later.

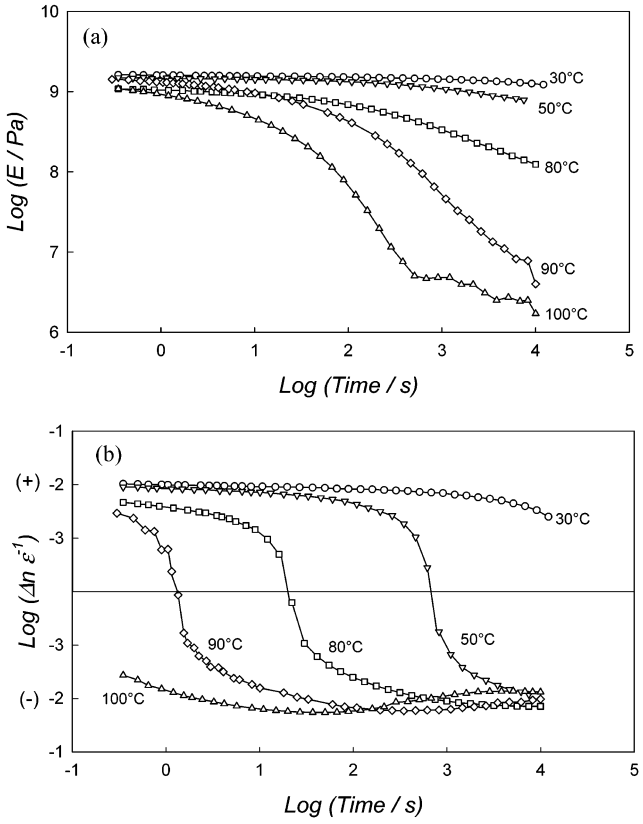

Figure 2. Time dependence of relaxation modulus $E(t)$ (a) and relaxation birefringence $\Delta n(t)/\epsilon$ (b) of SAN at various temperatures.

Figure 4 shows the time dependence of the birefringence $\Delta n(t)/\epsilon$ when the stress was released, and the specimen was cooled to 30 °C after the stress relaxation. Here, the arrow shows the time when the stress was released and the specimen was cooled. The Δn changed sign from positive to negative after the stress release at 60 °C. On the other hand, the value of the negative Δn became larger after the stress release at 90 °C. These results suggest that the Δn could not be frozen by cooling, and it could not be recovered to the unloaded value by releasing the stress. This may be ascribed to the existence of the two molecular mechanisms; i.e., the Δn consists of distortion birefringence and orientation one.[1−4] Assuming that the distortion birefringence is positive while the orientation birefringence is negative, the Δn is positive when the distortion birefringence is larger than the orientation one while it is negative when the distortion birefringence is smaller than the orientation one. When the distortion is recovered after releasing the stress while the orientation is frozen by cooling, the positive Δn changes to negative one by recovering the large positive distortion birefringence and freezing the small negative orientation one, as observed after stress relaxation at 60 °C. On the other hand, the value of the negative Δn becomes larger by recovering the small positive distortion birefringence and freezing the large

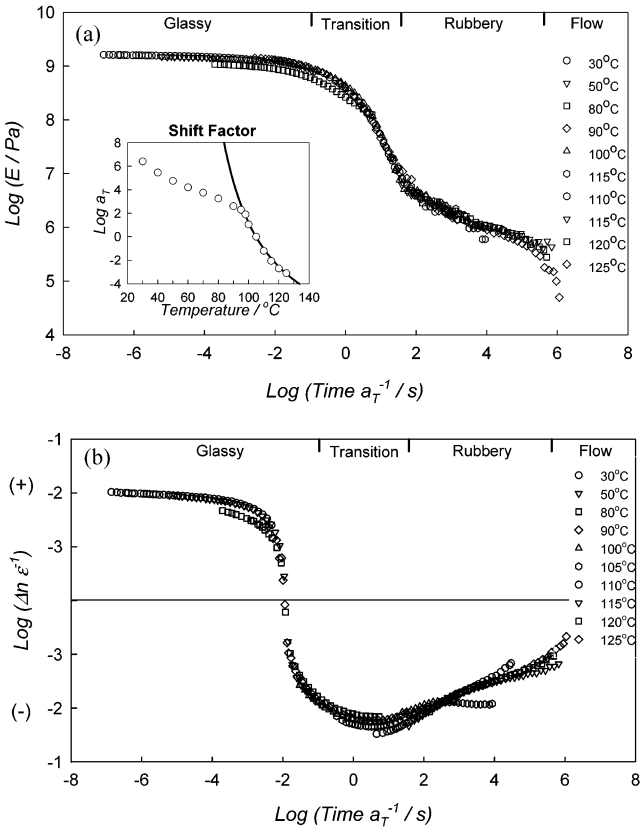

Figure 3. Master curves of relaxation modulus $E(t/a_T)$ (a) and relaxation birefringence $\Delta n(t/a_T)/\epsilon$ (b) of SAN; reduced at 105 °C.

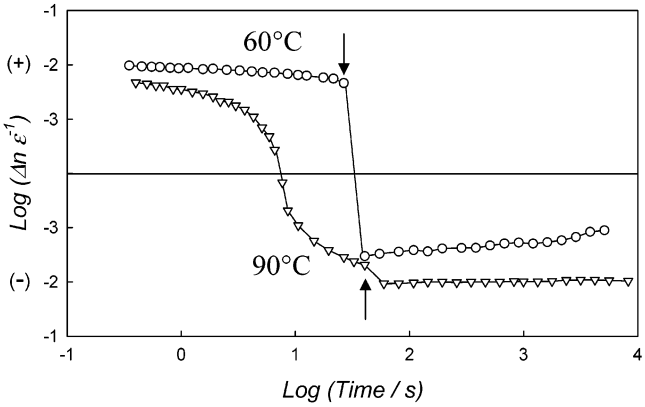

Figure 4. Time dependence of the birefringence $\Delta n(t)/\epsilon$ of SAN when the stress was released and the specimen was cooled to 30 °C after the stress relaxation at various temperatures. The arrow shows the time when the stress was released and the specimen was cooled.

negative orientation one, as observed after stress relaxation at 90 °C.

The distortion birefringence and orientation one can be characterized more quantitatively by analyzing both relaxation modulus $E(t/a_T)$ and relaxation birefringence $\Delta n(t/a_T)/\epsilon$. According to Read[1] and Inoue et al.,[27] the $E(t/a_T)$ and $\Delta n(t/a_T)/\epsilon$ are given by the sum of the distortional and orientational contributions:

$$E(t/a_T) = E_d(t/a_T) + E_o(t/a_T) \quad (3)$$

$$\Delta n(t/a_T)/\epsilon = \Delta n_d(t/a_T)/\epsilon + \Delta n_o(t/a_T)/\epsilon = C_d E_d(t/a_T) + C_o E_o(t/a_T) \quad (4)$$

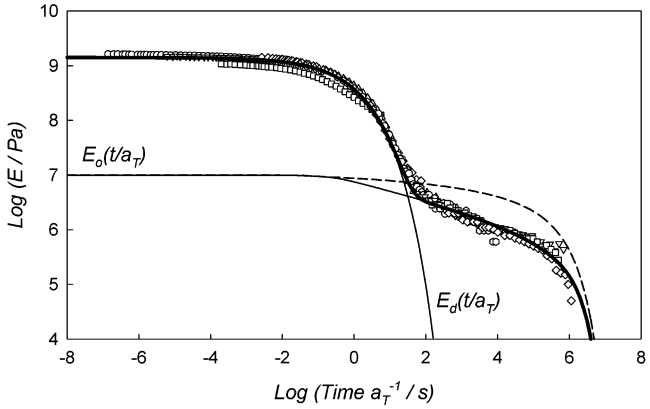

Figure 5. Calculated curves of $E_d(t/a_T)$, $E_o(t/a_T)$, and $E(t/a_T)$ of SAN by eqs 3, 5, and 6: $E_{d,max} = 1.4 \times 10^9$ Pa, $\tau_d = 0.5$ s, $\beta = 0.43$, $E_{o,max} = 3.2 \times 10^5$ Pa, $\tau_o = 0.1$ s, $\alpha = 0.7$, $n_e = 150$, and $n = 2000$. The broken line was calculated by the Doi−Edwards equation.

where subscripts d and o are distortional and orientational contributions to the $E(t/a_T)$ and $\Delta n(t/a_T)/\epsilon$, respectively, and C_d and C_o are stress−optical coefficients for distortion and orientation, respectively.

The relaxation of the distortion modulus $E_d(t/a_T)$ may be described by the Kohlrausch−Williams−Watts (KWW) equation, which is often used to explain the stress relaxation behavior in the glassy region:[28,29]

$$E_d(t) = E_{d,max} \exp\left\{-\left(\frac{t}{\tau_d}\right)^{\beta}\right\} \quad (5)$$

where τ_d is the relaxation time of distortion and β is the distribution parameter for the relaxation time of the distortion. On the other hand, the relaxation of the orientation modulus $E_o(t/a_T)$ may be described by the modified Rouse equation:[30]

$$E_o(t) = E_{o,max} \sum_{p=1}^{n-1} \frac{1}{p^{\alpha}} \exp\left(-\frac{t}{2\tau_o} \frac{1}{1 + n/n_e} \frac{p^2\pi^2}{n^2}\right) \quad (6)$$

where τ_o is the relaxation time of orientation, α is the distribution parameter for the relaxation time of the orientation, n is the number of segments, and n_e is the n between dynamic entanglements. The modified Rouse model assumes that (1) the interest chain behaves like a Rouse chain, (2) the interest chain motion is restricted and dragged by the surrounding chains due to the entanglements, and (3) the entanglements behave like the slow moving points in the interest chain.[30]

Figure 5 shows the calculated curves of the $E(t/a_T)$ obtained by eqs 3, 5, and 6. The steep decrease of the $E(t/a_T)$ in the glass transition region can be explained by the KWW equation, as shown by the curve of the $E_d(t/a_T)$ in Figure 5. On the other hand, the slight decrease in the plateau region can be explained by the modified Rouse equation, as shown by the curve of the $E_o(t/a_T)$ in Figure 5. Note here that the plateau region in the $E_o(t/a_T)$ calculated by the Doi−Edwards equation[31−33] is too flat to explain the decrease of the $E(t/a_T)$, as shown by the broken line in Figure 5. The glass transition region becomes wider and shifts to shorter time by assuming smaller β and smaller τ_d. As the α is smaller, the slope of the plateau region becomes steeper. The plateau region shifts to shorter time as the τ_o is smaller. We selected the best set of the above parameters to fit the calculated $E(t/a_T)$ curve to the observed

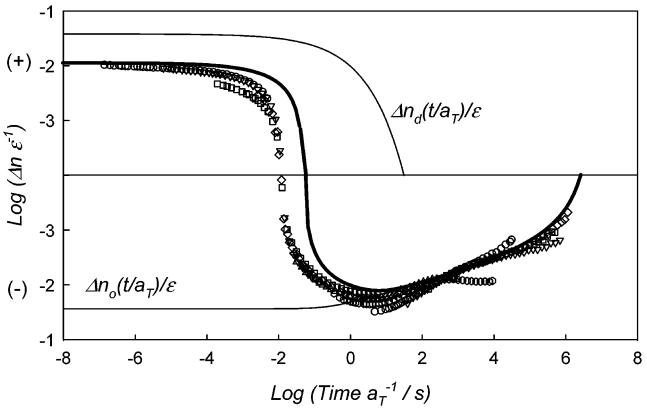

Figure 6. Calculated curves of $\Delta n_d(t/a_T)/\epsilon$, $\Delta n_o(t/a_T)/\epsilon$, and $\Delta n(t/a_T)/\epsilon$ of SAN by eqs 3−6: $C_d = 2.7 \times 10^{-11}$ Pa^{-1}, $C_o = -2.8 \times 10^{-9}$ Pa^{-1}, $\tau_d = 0.5$ s, $\beta = 0.43$, $\tau_o = 0.1$ s, $\alpha = 0.7$, $n_e = 150$, and $n = 2000$.

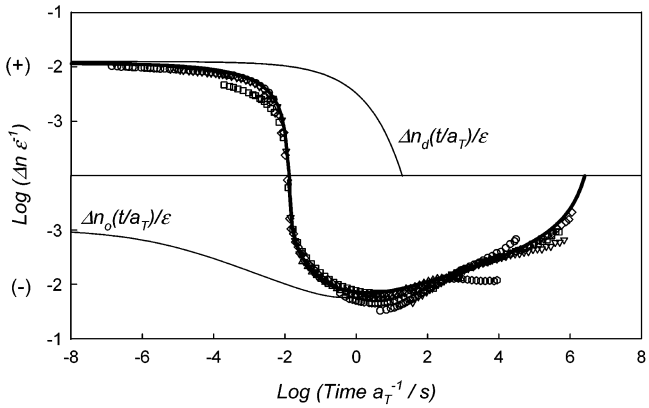

Figure 7. Calculated curves of $\Delta n_d(t/a_T)/\epsilon$, $\Delta n_o(t/a_T)/\epsilon$, and $\Delta n(t/a_T)/\epsilon$ of SAN by eqs 3−7: $C_d = 8.9 \times 10^{-12}$ Pa^{-1}, $C_o = -2.8 \times 10^{-9}$ Pa^{-1}, $C_g = 2.7 \times 10^{-9}$ Pa^{-1}, $\tau_p = 0.15$ s, $\gamma = 0.32$, $\tau_d = 0.5$ s, $\beta = 0.43$, $\tau_o = 0.1$ s, $\alpha = 0.7$, $n_e = 150$, and $n = 2000$.

one, as shown by the solid line in Figure 5. The E_d is larger than the E_o in the glassy region, and the E_d relaxes faster than the E_o. This may explain the steep inflection at the onset t/a_T of the plateau region.

The calculated curves of the $\Delta n(t/a_T)/\epsilon$ obtained by eqs 3−6 are shown in Figure 6. As demonstrated in Figure 4, the distortion birefringence is positive while the orientation birefringence is negative; i.e., the C_d is positive while the C_o is negative. Since the C_d is positive while the C_o is negative and the Δn_d ($=E_dC_d$) relaxes faster than the Δn_o ($=E_oC_o$), the calculated curve changes the sign from positive to negative by assuming that the absolute value of the Δn_d is larger than that of the Δn_o in the glassy region. Though the inflection at the onset t/a_T of the plateau region is large in the $E(t/a_T)$ due to large E_d/E_o in the glassy region (see Figure 5), the inflection is small in the $\Delta n(t/a_T)/\epsilon$ when $\Delta n_d/\Delta n_o$ ($=E_dC_d/E_oC_o$) is small due to small C_d/C_o. However, the calculated $\Delta n(t/a_T)/\epsilon$ is far from the observed one; i.e., the onset t/a_T for the change in the sign of the $\Delta n(t/a_T)/\epsilon$ is different. The deviation suggests an additional contribution to the $\Delta n(t/a_T)/\epsilon$. This may be ascribed to the change in the C_o with t/a_T due to the conformational change of the phenyl ring side group.

Taking into account the conformational change during the stress relaxation, the C_o may be modified by a stretched exponential relaxation function:

$$C_o' = C_o + C_g \exp\left\{-\left(\frac{t}{\tau_p}\right)^{\gamma}\right\} \qquad (7)$$

where τ_p is the relaxation time for the conformational change of the phenyl ring side group, γ is the distribution parameter for the relaxation time of the conformational change, and C_g is the contribution of the conformational change to the C_o. The $\Delta n_o(t/a_T)/\epsilon$ calculated by eqs 6 and 7 is shown in Figure 7. The $\Delta n_o(t/a_T)/\epsilon$ changes with t/a_T in the glassy region at $t/a_T < 0$ by assuming the modified stress−optical coefficient C_o' and $\tau_p < 1$ s. As shown by the solid line in Figure 7, the observed $\Delta n(t/a_T)/\epsilon$ curve could be nicely explained by eqs 3−7. The relaxation time τ_p estimated by the fitting procedure was about 0.15 s at a reference temperature of 105 °C. The result suggests that the conformational change is much slower than the phenyl ring vibration (β-relaxation) in which the relaxation time is 10^{-4} s at 50 °C.

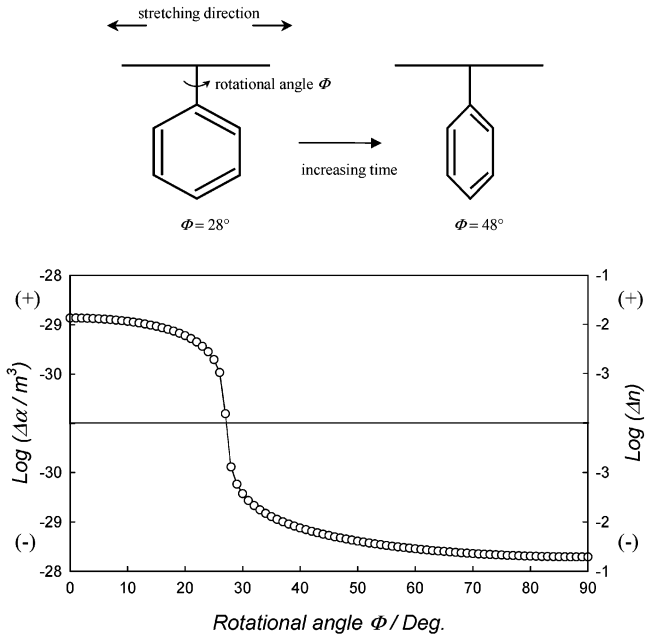

Figure 8. Schematic representation of the conformational change of phenyl ring side group and change of the polarizability difference Δa with rotational angle Φ.

Figure 8 shows the schematic representation of the conformational change of the phenyl ring side group. As demonstrated by Gurnee,[34] the polarizability difference $\Delta\alpha$ changes by the conformational change of the phenyl ring side group which is accompanied by the change of the rotational angle between the phenyl ring plane and the main-chain axis. The $\Delta\alpha$ is given by

$$\Delta\alpha = \alpha_X - (\alpha_Y + \alpha_Z)/2 \qquad (8)$$

where α_i is the principal polarizability of monomer. α_i is represented as a sum of contributions from its constituent bonds. One can estimate the contribution from the individual bond using the transformation of the polarizability tensor $(\alpha)_{X'Y'Z'}$ for the $(X'Y'Z')$ coordinate of a constituent bond into the (XYZ) coordinate of the chain axis by

$$(\alpha)_{XYZ} = R_Z(\theta)\, R_{X'}(\phi)\, \mathrm{diag}(\alpha)_{X'Y'Z'}\, R_{X'}(\phi)^{-1}\, R_Z(\theta)^{-1} \qquad (9)$$

$$R_{X'}(\phi) = \begin{pmatrix} 1 & 0 & 0 \\ 0 & \cos\phi & -\sin\phi \\ 0 & \sin\phi & \cos\phi \end{pmatrix}$$

$$R_Z(\theta) = \begin{pmatrix} \cos\theta & -\sin\theta & 0 \\ \sin\theta & \cos\theta & 0 \\ 0 & 0 & 1 \end{pmatrix} \quad (10)$$

where $R_{X'}(\phi)$ is the transformation for a rotation ϕ of the bond about the X' axis and $R_Z(\theta)$ is that for a rotation θ about the Z axis.[35−37]

The $\Delta\alpha$ of SAN calculated by eqs 8−10 is shown in the lower part of Figure 8 as a function of the rotational angle Φ of the phenyl ring side group. The birefringence Δn is approximately related to the polarizability difference $\Delta\alpha$ by differentiating the Lorentz−Lorenz equation.[37] The Δn thus obtained is also shown in the lower part of Figure 8. The Δn decreases and changes the sign from positive to negative, and the negative value increases with increasing the rotational angle Φ. As demonstrated in Figure 7, the Δn_o changes from $-10^{-2.9}$ to $-10^{-1.8}$ with increasing the t/a_T from 10^{-8} to 1 s. The Φ is 28° when the Δn_o is $-10^{-2.9}$, and it is 48° when the Δn_o is $-10^{-1.8}$. Thus, the results suggest that the Φ changes from 28° at $t/a_T = 10^{-8}$ s to 48° at $t/a_T = 1$ s due to the conformational change of the side group with a relaxation time of 0.15 s (at 105 °C) during the stress relaxation.

Conclusion

The birefringence of SAN changed its sign from positive to negative during the stress relaxation in the glassy state. The value of the negative birefringence was found to increase when the stress was released, and the specimen was cooled to room temperature. Such characteristic birefringence behavior is ascribed to the distortion relaxation and the conformational change of the phenyl ring side group associating with the orientation relaxation. The curve fitting procedures of the stress and birefringence relaxation curves revealed that the conformational change of the side group is much slower than the phenyl ring vibration (β-relaxation).

References and Notes

(1) Read, B. E. *Polym. Eng. Sci.* **1983**, *23*, 835.
(2) Yannas, I. V.; Luise, R. R. *J. Macromol. Sci., Phys.* **1982**, *B21*, 443.
(3) Koenen, J. A.; Heise, B.; Killian, H. G. *J. Polym. Sci., Polym. Phys. Ed.* **1989**, *27*, 1235.
(4) Priss, L. S.; Vishnyakov, I. I.; Pavlova, I. P. *Int. J. Polym. Mater.* **1980**, *8*, 85.
(5) Tanaka, T.; Inoue, T. *J. Non-Cryst. Solids* **1991**, *131−133*, 781.
(6) Nagasawa, M.; Koizuka, A.; Matsuura, K.; Horita, M. *Macromolecules* **1990**, *23*, 5079.
(7) Shimo, T.; Nagasawa, M. *Macromolecules* **1992**, *25*, 5026.
(8) Rudd, J. F.; Andrews, R. D. *J. Appl. Phys.* **1960**, *31*, 818.
(9) Kolsky, H. *Nature (London)* **1950**, *166*, 235.
(10) Illers, K. H.; Jenckel, E. *J. Polym. Sci.* **1959**, *41*, 528.
(11) Seefried, C. G., Jr.; Koleske, J. V. *J. Polym. Sci., Polym. Phys. Ed.* **1976**, *14*, 663.
(12) Yano, O.; Wada, Y. *J. Polym. Sci., Part A2* **1971**, *9*, 669.
(13) Yano, O.; Wada, Y. *J. Polym. Sci., Polym. Phys. Ed.* **1974**, *12*, 665.
(14) Zhao, J.; Chin, Y. H.; Liu, Y.; Jones, A. A.; Inglefield, P. T.; Kambour, R. P.; White, D. M. *Macromolecules* **1995**, *28*, 3881.
(15) Kulik, A. S.; Prins, K. O. *Polymer* **1993**, *34*, 4635.
(16) Spiess, H. W. *Colloid Polym. Sci.* **1983**, *261*, 193.
(17) Spiess, H. W. *J. Mol. Struct.* **1983**, *111*, 119.
(18) Schaefer, J.; Sefcik, M. D.; Stejskal, E. O.; McKay, R. A.; Dixon, W. T.; Cais, R. E. *Macromolecules* **1984**, *17*, 1107.
(19) Kanaya, T.; Kawaguchi, T.; Kaji, K. *J. Non-Cryst. Solids* **1994**, *172−174*, 327.
(20) Kanaya, T.; Kawaguchi, T.; Kaji, K. *Physica B* **1995**, *213−214*, 510.
(21) Modine, F. A.; Major, R. W.; Sonder, E. *Appl. Opt.* **1975**, *14*, 757.
(22) Kornfield, J. A.; Feller, G. G.; Pearson, D. S. *Macromolecules* **1989**, *22*, 1334.
(23) Saito, H.; Miyashita, H.; Inoue, T. *Macromolecules* **1992**, *25*, 1824.
(24) Fulcher, G. A. *J. Am. Ceram. Soc.* **1925**, *8*, 339.
(25) Perez, J.; Cavaille, J. Y. *J. Non-Cryst. Solids* **1994**, *172−174*, 1028.
(26) Hoffman, A.; Kremer, F.; Fischer, E. W.; Schonhals, A. In *Disorder Effects on Relaxation Process, Glass, Polymer, Proteins*; Richter, R., Blumen, A., Eds.; Springer: Berlin, 1994.
(27) Inoue, T.; Okamoto, H.; Osaki, K. *Macromolecules* **1991**, *24*, 5670.
(28) Williams, G.; Watts, D. C. *Trans. Faraday Soc.* **1971**, *67*, 1323.
(29) Matsuoka, S. *Relaxation Phenomena in Polymers*; Hanser: New York, 1992.
(30) Skolnick, J.; Yaris, R. T. *J. Chem. Phys.* **1988**, *88*, 1418.
(31) Doi, M.; Edwards, S. F. *J. Chem. Soc., Faraday Trans. 2* **1978**, *74*, 1802.
(32) Doi, M.; Edwards, S. F. *The Theory of Polymer Dynamics*; Clarendon: Oxford, 1986.
(33) The Doi−Edwards model is familiar to explain the modulus relaxation and molecular motion in the rubbery plateau region. This model assumes reptation motion in the tube which consists of the entanglements due to the matrix of chains surrounding the interest chain. The $E_o(t/a_T)$ is described by the Doi−Edwards model: $E_o(t) = E_{o,max}\sum_{p=1}^{n-1}(1/p^\alpha)\exp[-t/(\tau_o/p^\delta)]$.
(34) Gurnee, E. F. *J. Appl. Phys.* **1954**, *25*, 1232.
(35) Smith, R. P.; Mortensen, E. M. *J. Chem. Phys.* **1960**, *32*, 502.
(36) Erman, B.; Marvin, D. C.; Irvine, P. A.; Flory, P. J. *Macromolecules* **1982**, *15*, 664.
(37) Saito, H.; Inoue, T. *J. Polym. Sci., Polym. Phys.* **1987**, *25*, 1629.

MA035458A